

Periodic change in absorption maxima due to different chain packing between the bilayers of amphiphiles possessing even and odd numbers of carbons in the hydrophobic chain

Norihiro Yamada,^a Kenji Okuyama,^b Takeshi Serizawa,^a Masashi Kawasaki^a and Shinichiro Oshima^b

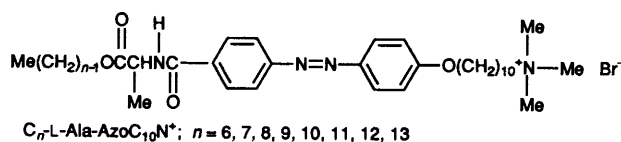
^a Faculty of Education, Chiba University, Yayoi-cho, Inage-ku, Chiba, 263, Japan

^b Faculty of Technology, Tokyo University of Agriculture and Technology, Koganei, Tokyo 184, Japan

N-{4-[4-(10-Trimethylammoniododecyloxy)phenylazo]benzoyl}-L-alanine alkyl ester bromides with *n*-C₆ to -C₁₃ alkyl chains have been newly synthesized. The bilayer aggregates absorbed at 355 nm when the number of carbons was even and at 320 nm when odd. Regardless of whether the number was even or odd, X-ray diffraction patterns suggested a chain penetration structure, where the tail chains in one molecular layer penetrated into the opposite molecular layer, and hence every other azobenzene group was distributed into the opposite layers. However, a remarkable splitting of the CH₂ scissoring band into 1473 and 1463 cm⁻¹ indicated perpendicular alignments of the *trans*-zigzag planes of the chains containing an even number of carbons, whereas the singlet CH₂ scissoring band at 1465 cm⁻¹ indicated parallel alignments of the planes of the chains containing an odd number of carbons. In accord with the chain packing, when the amphiphiles possess an even number of carbons, the adjacent neighbouring azobenzenes in each layer were arranged perpendicular to each other. The perpendicular location causes a loss of interchromophore interaction, giving λ_{max} at 355 nm. In contrast, the azobenzenes in the bilayers of the amphiphiles containing an odd number of carbons were all parallel to each other. Because the molecules were tilted above about 60°, a H aggregate should be predominantly formed, which absorbed at 320 nm. In addition, the amphiphiles containing an even number of carbons formed stronger H bonding than those containing an odd number of carbons.

Introduction

Regardless of whether they are natural or artificial, amphiphiles self-organize into a bilayer membrane. Since Kunitake and Okahata established the self-assembling concept,¹ many kinds of artificial amphiphiles have been synthesized and characterized to constitute a new molecular architecture system.² However, we can scarcely find a study on amphiphiles which possess an odd number of carbon atoms in the hydrophobic chain. We thus synthesized and characterized amphiphiles possessing not only an even, but also an odd number of carbons in the tail, particularly azobenzene-containing amphiphiles such as *N*-{4-[4-(10-trimethylammoniododecyloxy)phenylazo]benzoyl}-L-alanine alkyl ester bromide, which we called C_{*n*}-L-Ala-Azo-C₁₀N⁺. These amphiphiles contain an azobenzene group, an alaninate residue and a long tail chain including 6–13 carbon atoms. The general formula is shown below.



Previously, we reported that the amphiphile of C₁₂-L-Ala-Azo-C₁₀N⁺ immediately formed micellar fibres in water, and they were transformed into helical superstructures† within 24 h

† The helical superstructure is known to possess a bilayer structure (see ref. 2 and other references cited therein). The extraordinary morphology is maintained only in the crystalline state of the bilayers. All the amphiphiles used in this work formed the helical superstructure by incubation as briefly described in a preliminary report.³ The even-odd-chain effect in the present study was observed only when the helix-formation was completed.

at room temperature.³ The morphological transformation was accompanied by a λ_{max} shift from 320 to 350 nm. The peculiar red shift is common to the aqueous dispersions of the amphiphiles containing an even number of carbons, whereas the aqueous dispersions of the amphiphiles containing an odd number of carbons absorbed at *ca.* 320 nm and displayed no spectral change even if a morphological transformation occurred. Hence the absorption maximum alternately changes with the number of carbons in the hydrophobic chain. In addition, the crystal-to-liquid crystal phase transition temperature (*T_c*) also alternates with the number of carbons. A brief preliminary report of this work has appeared elsewhere.⁴

The aforementioned spectral difference is apparently derived from the different orientation of the chromophores. The stacking modes of the chromophores within bilayers of azobenzene-containing amphiphiles have been classified into four categories:⁵ (i) the H aggregate (*ca.* 300 nm), where the azobenzene planes are all parallel to each other, and every long axis of the chromophore is approximately vertical to the membrane plane; (ii) the less-stacked structure (330–340 nm), which is observed for some of the bilayers in the liquid-crystalline state; (iii) the monomeric dispersion (355 nm), where the chromophores are rotationally disordered or isolated from each other; and (iv) the J aggregate (360–390 nm), where the azobenzene planes are all parallel to each other, and every long axis of the chromophore is greatly tilted within the membrane. According to the classification, the bilayers of the amphiphiles containing an odd number of carbons should undoubtedly form the H aggregate. However, we cannot explain a structure within the bilayer of the amphiphiles containing an even number of carbons, because the λ_{max} at 350 nm is close to that given by the isolated structure in (iii), which has never been observed within bilayers in the crystalline state.

The main emphasis of this study will be on the structural aspects of the peculiar red shift within the bilayers of the

amphiphiles containing an even number of carbons. We investigated the aggregation structure of the cast film bilayers of C_n -L-Ala-Azo- C_{10} - N^+ using Fourier transform infrared (FTIR) spectroscopy and X-ray diffraction, because it is known that the structure and properties are maintained in an air-dried cast film from an aqueous dispersion.⁶ The thickness of the bilayer membrane, the mode of the intermolecular hydrogen bonding and chain packing will become apparent with these experiments. The other main purpose of this study was to concentrate on the previously neglected amphiphiles containing an odd number of carbons. It is known that the thermal behaviour and crystal structures of the long chain compounds such as alkanes⁷ and fatty acids⁸ are entirely different between the species containing an even and odd number of carbons. The difference could be reflected in the bilayer characteristics because the long chain compound is an essential module of bilayer-forming amphiphiles.

Experimental

Compounds

L-Alanine, long chain alcohols and 1,10-dibromodecane were commercially available (Wako Pure Chemical Ind., Ltd). 4-(4-Hydroxyphenylazo)benzoic acid was prepared by the method described elsewhere.⁹ The preparation method for C_6 -L-Ala-Azo- C_{10} - N^+ was reported by Nakashima *et al.*¹⁰ Some modifications were made in the syntheses of C_n -L-Ala-Azo- C_{10} - N^+ . As an example, the procedure for the synthesis of C_{11} -L-Ala-Azo- C_{10} - N^+ is given below.

Undecyl-L-alaninate hydrochloride. A mixture of L-alanine (1.6 g, 18 mmol), undecan-1-ol (3.1 g, 18 mmol) and *p*-toluenesulfonate monohydrate (3.8 g, 20 mmol) in 100 ml of toluene was refluxed until the calculated amount of water was collected in the Dean and Stark water trap.¹¹ The mixture was condensed to dryness under reduced pressure. The residual oil containing undecyl L-alaninate *p*-toluenesulfonate was dissolved in chloroform, washed with 10% sodium carbonate and with water, dried over $MgSO_4$ and evaporated to obtain a colourless oil containing undecyl L-alaninate. Undecyl L-alaninate was neutralized by a minimal amount of conc. HCl in acetone. The solvents were evaporated *in vacuo* and the residual solid was recrystallized four times from acetone to give colourless undecyl-L-alaninate hydrochloride (3.0 g, 60%), mp 101.6–104.6 °C; $\nu_{max}(CCl_4 \text{ paste})$ 3400–2500br ($-N^+H_3$) and 1740vs cm^{-1} (ester).

The other alkyl-L-alaninate hydrochlorides were prepared in the same manner described above. Because hexyl L-alaninate hydrochloride does not crystallize, hexyl-L-alaninate *p*-toluenesulfonate was used without further treatment. All the alkyl alaninates were colourless powders and gave mostly the same IR spectra. All the melting points of these alaninates are summarized in Table 1.

4-[4-(10-Bromodecyloxy)phenylazo]benzoic acid. Into a

Table 1 Melting points of the intermediates

| <i>n</i> | C_n -L-Ala-HCl | | C_n -L-Ala-Azo- C_{10} -Br | |
|----------|------------------|-----------|--------------------------------|-------------|
| | Mp/°C | Yield (%) | Solvent | Mp/°C |
| 6 | oil | 65 | Hexane | 94.5–105 |
| 7 | 69.1–98.1 | 65 | MeOH | 101.2–104.0 |
| 8 | 99.5–100.5 | 68 | MeOH | 100.8–109.0 |
| 9 | 102.2–103.2 | 18 | MeOH | 105.6–107.0 |
| 10 | 100.5–101.5 | 32 | Me ₂ CO | 97.0–99.0 |
| 11 | 101.6–104.6 | 60 | EtOH | 103.0–106.9 |
| 12 | 105.0–106.0 | 52 | Me ₂ CO | 92.0–95.0 |
| 13 | 105.7–107.6 | 67 | Me ₂ CO | 102.8–106.5 |

solution of potassium ethoxide, prepared by dissolving potassium hydroxide (85% purity, 1.3 g, 20 mmol) in 100 ml of ethanol, 4-(4-hydroxyphenylazo)benzoic acid (2.4 g, 9.9 mmol) and 1,10-dibromodecane (4.0 g, 13 mmol) were dissolved in that order. The mixture was refluxed for 20 h, cooled to room temperature and filtered to obtain the crude product together with KBr. With the addition of 1 ml of conc. HCl, the crude product was dissolved in tetrahydrofuran (THF). The mixture was filtered to remove precipitates of KBr and evaporated to dryness under reduced pressure. The orange solids thus obtained were recrystallized twice from a minimal amount of THF and methanol (1.9 g, 42%), mp 150.0–228.0 °C (decomp.) (lit.,¹⁰ 195.0–225 °C, decomp.); $\nu_{max}(CCl_4 \text{ paste})$ 2900s ($\nu_{as} CH_2$), 2830s ($\nu_s CH_2$), 1670vs and 1245s cm^{-1} (ether).

Undecyl *N*-{4-[4-(10-bromodecyloxy)phenylazo]benzoyl}-L-alaninate. Into a mixture of 4-[4-(10-bromodecyloxy)phenylazo]benzoic acid (0.9 g, 2.0 mmol) and undecyl-L-alaninate hydrochloride (0.6 g, 2.1 mmol) in 50 ml of dry THF, Et₃N (0.7 g, 6.9 mmol) was added at once. Et₃N HCl immediately precipitated. Whilst stirring, a solution of diethyl phosphorocyanidate (1.7 g, 10 mmol) in 10 ml of dry THF was added within 15 min at a temperature below 5 °C. the mixture was allowed to stand overnight at room temperature, filtered and evaporated to dryness *in vacuo*. The residual orange solids were dissolved in chloroform, washed with salt water, evaporated and recrystallized twice from ethanol to give an orange powder (0.8 g, 60%), mp 103.0–106.9 °C; $\nu_{max}(CCl_4 \text{ paste})$ 3280s (NH), 2910vs ($\nu_{as} CH_2$), 2840s ($\nu_s CH_2$), 1740vs (ester), 1630vs (amide I), 1530s (amide II), 1240s (ether) and 1200vs cm^{-1} (ester).

The other compounds were synthesized in the same manner. The yields, the recrystallization solvents and the melting points are summarized in Table 1.

Undecyl *N*-{4-[4-(10-trimethylammoniododecyloxy)phenylazo]benzoyl}-L-alaninate bromide. In this procedure, simultaneous use of an amine trap and a hood was required because Me₃N has an extremely bad odour. Undecyl *N*-{4-[4-(10-bromodecyloxy)phenylazo]benzoyl}-L-alaninate (0.75 g, 1.1 mmol) was dissolved in 100 ml of dry THF. Dry Me₃N gas was bubbled into the solution under vigorous stirring with ice cool-

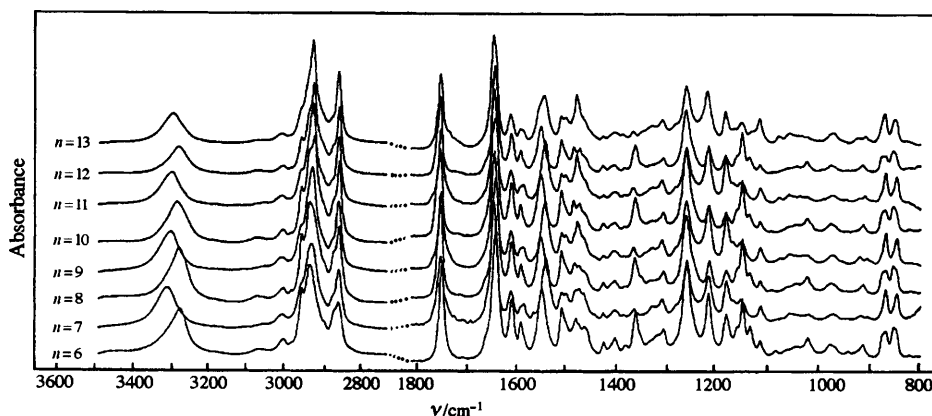
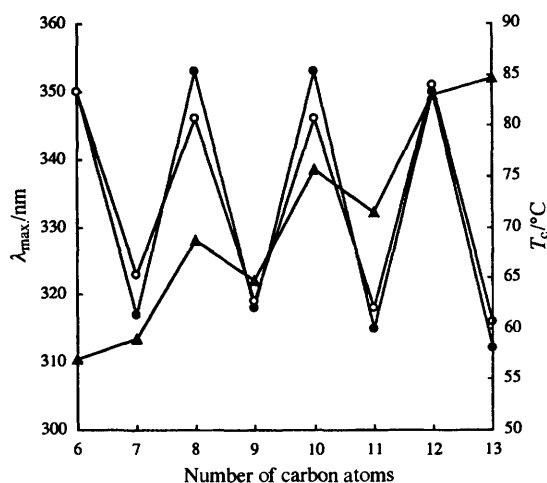


Fig. 1 FTIR spectra of the cast film bilayers of C_n -L-Ala-Azo- C_{10} - N^+

Table 2 Analytical data for the C_n -L-Ala-Azo- $C_{10}N^+$

| Compound (Formula) | Yield (%) | Solvent | Mp/°C | Found (%) (Required) | | |
|---|-----------|---------------------------|-------------|-------------------------|----------------|----------------|
| | | | | C | H | N |
| C_6 -Ala-Azo- $C_{10}N^+$ $C_{35}H_{55}N_4O_4Br \cdot 0.3H_2O$ | 16 | MeOH– Ether | 124.0–127.0 | 61.72 (61.72) | 8.13 (8.23) | 8.22 (8.23) |
| C_7 -Ala-Azo- $C_{10}N^+$ $C_{36}H_{57}N_4O_4Br \cdot 0.55H_2O$ | 27 | Me ₂ CO– Ether | 128.0–129.5 | 61.80 (61.80) | 8.17 (8.37) | 7.97 (8.01) |
| C_8 -Ala-Azo- $C_{10}N^+$ $C_{37}H_{59}N_4O_4Br \cdot 0.55H_2O$ | 31 | Me ₂ CO– Ether | 133.5–135.5 | 62.24 (62.27) | 8.29 (8.49) | 7.80 (7.85) |
| C_9 -Ala-Azo- $C_{10}N^+$ $C_{38}H_{61}N_4O_4Br \cdot 0.50H_2O$ | 31 | Me ₂ CO | 125.5–133.5 | 63.00 (62.86) | 8.55 (8.60) | 7.68 (7.71) |
| C_{10} -Ala-Azo- $C_{10}N^+$ $C_{39}H_{63}N_4O_4Br \cdot 0.50H_2O$ | 46 | CHCl ₃ – Ether | 133.7–134.8 | 61.84 (61.73) | 8.45 (8.77) | 7.35 (7.38) |
| C_{11} -Ala-Azo- $C_{10}N^+$ $C_{40}H_{65}N_4O_4Br \cdot 0.50H_2O$ | 25 | CHCl ₃ – Ether | 136.0–139.2 | 63.59 (63.64) | 8.69 (8.81) | 7.43 (7.42) |
| C_{12} -Ala-Azo- $C_{10}N^+$ $C_{41}H_{67}N_4O_4Br \cdot 0.50H_2O$ | 49 | MeOH– Ether | 134.0–135.0 | 61.72 (61.72) | 8.13 (8.23) | 8.22 (8.23) |
| C_{13} -Ala-Azo- $C_{10}N^+$ $C_{42}H_{69}N_4O_4Br \cdot 1.00H_2O$ | 36 | Me ₂ CO | 139.5–147.0 | 63.89 (63.70) | 8.66 (8.78) | 7.02 (7.08) |

**Fig. 2** Periodic changes in the absorption maxima and T_c for the bilayer membranes of C_n -L-Ala-Azo- $C_{10}N^+$; ●, aqueous dispersions; ○, cast films; ▲, T_c of the aqueous dispersions

ing until the total volume of the solution slightly increased. The flask was stoppered and allowed to stand for 1 week at room temperature in the dark. The solvent and excess Me₃N were removed under reduced pressure. The residual orange solid was recrystallized three times from a chloroform–diethyl ether mixture and then from acetone (0.2 g, 25%), mp 136.0–139.2 °C (Found; C, 63.59; H, 8.69; N, 7.43. Calc. for $C_{40}H_{65}N_4O_4Br \cdot 0.5H_2O$: C, 63.64; H, 8.81; N, 7.42%); ν_{max} (CCl₄ paste) 3400br (H₂O), 3300s (NH), 2910vs (ν_{as} CH₂), 2840s (ν_s CH₂), 1740vs (ester), 1630vs (amide I), 1530s (amide II), 1245s (ether) and 1200vs cm⁻¹ (ester); ν_{max} (cast film from aqueous dispersion) is given in Fig. 1; δ_H (100 MHz; solvent CDCl₃; standard Me₄Si) 0.90 (3 H, br t, CH₂CH₃), 1.25 (34 H, s, CH₂CH₂CH₂), 1.55 (3 H, d, CHCH₃), 3.47 (11 H, s, CH₂NCH₃), 3.9–4.5 (4 H, br m, OCH₂), 4.5–5.2 (1 H, br m, CH), 6.9 (1 H, d, NH), 7.04 (2 H, d, N–Ph–O), 7.94 (2 H, d, N–Ph–O), 7.94 (4 H, s, C–Ph–N).

The other amphiphiles were prepared in the same manner as above. The melting points, the recrystallization solvents and the analytical data are given in Table 2.

Differential scanning calorimetry (DSC)

The T_c of the aqueous dispersions of C_n -L-Ala-Azo- $C_{10}N^+$ were determined using a SSC/560 thermal analyser manufactured by Seiko Instruments and Electronics, Ltd. The dispersion (60 μ l, 10 mm) was sealed in a 70 μ l silver pan. The DSC thermogram was recorded by heating the sample from 5 to 95 °C at the rate of 1 °C min⁻¹. A sealed silver pan including the same volume

Table 3 T_c and λ_{max} of the bilayer membranes of C_n -L-Ala-Azo- $C_{10}N^+$

| n | T_c /°C | λ_{max} /nm (20.0 \pm 0.5 °C) | |
|-----|-----------|---|------------|
| | | Aqueous dispersion | Cast films |
| 6 | 57.0 | 350 | 350 |
| 7 | 58.0 | 317 | 323 |
| 8 | 68.7 | 353 | 346 |
| 9 | 64.7 | 318 | 319 |
| 10 | 75.6 | 353 | 346 |
| 11 | 71.5 | 315 | 318 |
| 12 | 83.0 | 350 | 351 |
| 13 | 84.7 | 312 | 316 |

of water was used as a reference. The temperature at the top of the endothermic peak was adopted as the T_c . All the T_c values are listed in Table 3.

UV spectrophotometry

Aqueous dispersions (2 mm) prepared by sonication were allowed to stand at room temperature until the λ_{max} change terminated. A portion of the solution was uniformly spread on a quartz substrate and dried in the atmosphere at room temperature. If the cast film is prepared before the redshift from 320 to 350 nm has terminated in the original aqueous dispersion, the absorption maxima of the cast film contain both components. The UV spectra were obtained on a Hitachi U-3210 spectrometer at 20.0 \pm 0.5 °C. All the λ_{max} values are summarised in Table 3.

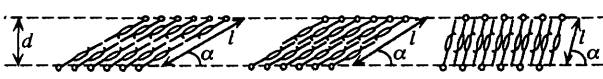
FTIR spectroscopy

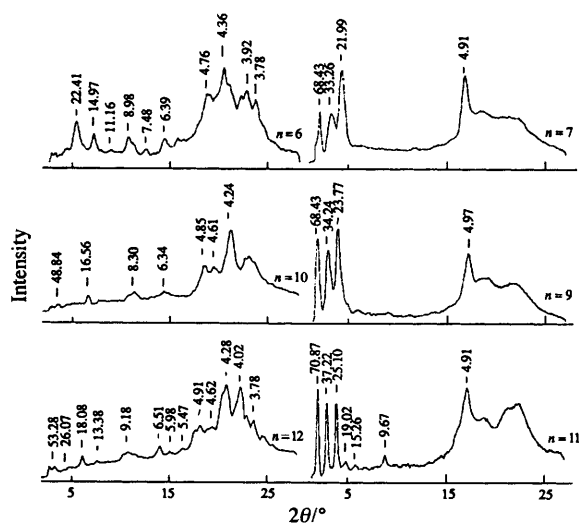
According to the method described above, cast films were prepared on the CaF₂ window. The CaF₂ window was mounted in a temperature-controlled flow-through cell (Harrick Scientific Co., TFC-M19). The IR spectra were recorded on a Nicolet 740 Fourier transform IR spectrometer with a TGS detector at 25 °C. Two hundred interferograms were co-added and Fourier transformed with one level of zero filling to yield spectra with a high signal-to-noise ratio at a resolution of 4 cm⁻¹.

X-Ray diffraction

Samples were ground to a fine powder using an agate mortar and pestle. The X-ray diffraction was carried out by the transmission method with a Rigaku Denki Rotaflex RU-200 X-ray generator and a Mac Science DIP-100 diffraction imaging plate at room temperature. The X-ray beam was generated with a Cu anode at 50 kV and 140 mA. The X-ray diffraction patterns were obtained by exposing the sample to monochromatized Cu-K α radiation through a collimator (0.5 mm) for 5 min.

Table 4 The observed bilayer thickness (d) and the tilt angle (α) of components within the three possible structures

| n | $d/\text{\AA}$ |  | | |
|-----|----------------|--|--|---|
| | | Classic bilayer structure α° ($//\text{\AA}$) | Chain penetration structure α° ($//\text{\AA}$) | Interdigitated structure α° ($//\text{\AA}$) |
| 6 | 44.8 | 33 (83.2) | 37 (75.2) | 67 (48.6) |
| 7 | 66.2 | 51 (85.6) | 60 (76.4) | ^a (49.8) |
| 9 | 69.5 | 50 (90.4) | 62 (78.8) | ^a (52.2) |
| 10 | 49.9 | 33 (92.8) | 39 (80.0) | 69 (53.4) |
| 11 | 75.8 | 53 (95.2) | 69 (81.2) | ^a (54.6) |
| 12 | 53.5 | 33 (98.4) | 40 (82.8) | 72 (56.2) |

^a Cannot calculate, see text.**Fig. 3** X-Ray diffraction patterns of C_n -L-Ala-Azo- $C_{10}N^+$ powder

Results

Overview of the even-odd-chain effect

We can readily obtain a cast film bilayer by drying an aqueous bilayer on an appropriate substrate. Because the drying process retains the original properties of the aqueous bilayer intact, the cast film which is easy to handle can be used for analysing the structure of the bilayer membranes. In fact, the cast films of C_n -L-Ala-Azo- $C_{10}N^+$ showed the same spectral change as observed in the original aqueous bilayers (Fig. 2). Fig. 2 shows that the amphiphiles containing an odd number of carbons form a highly ordered H aggregate (λ_{\max} 320 nm) despite the presence of the sterically hindered methyl group at the alaninate residue. On the other hand, the T_c values of the bilayers of amphiphiles containing an even number of carbons are higher than those estimated from the bilayers of amphiphiles containing an odd number of carbons (Fig. 2). The higher T_c value indicates closer packing of the chains; therefore, the bilayers of the amphiphiles containing an even number of carbons must possess an ordered structure of the chromophores. According to these results, regardless of the number of carbons, the amphiphiles should be arranged so as to avoid the steric hindrance of the methyl group and should form a highly ordered structure. The major problem is what kind of structure gives rise to the λ_{\max} at 350 nm.

X-Ray diffraction

We can calculate the thickness of the bilayer membranes of C_n -L-Ala-Azo- $C_{10}N^+$ from the small angle diffraction region in the X-ray diffraction patterns (Fig. 3). The membrane thickness (d) of the respective bilayer membranes are listed in Table 4. Because the extended molecular lengths calculated from the van der Waals model were 41.6 Å ($n=6$), 42.8 Å

($n=7$), 45.2 Å ($n=9$), 46.4 Å ($n=10$), 47.6 Å ($n=11$) and 49.2 Å ($n=12$), the observed membrane thicknesses were significantly smaller than the calculated bimolecular lengths. In particular, the bilayers of the amphiphiles containing an even number of carbons were very thin. By presuming a tilting bilayer structure, we can explain such thin bilayers. However, not only the angle of tilt but also the chain packing is different in each case. The wide angle diffraction regions between 3.5 and 5.5 Å are remarkably different depending on whether the number of carbons is even or odd. Hence, the aforementioned change in λ_{\max} and T_c must be considered not only based on the tilting of the molecules but also the chain packing. The details are discussed in the following section. However, it is known that each of the chain-packing subcells within the crystals of simple long chain compounds can be characterized by X-ray diffraction peaks in the wide-angle region.^{7,8} For example, the orthorhombic $O\perp$ and $O'\perp$ subcells [the symbol (\perp) indicates perpendicular] are characterized by two strong diffraction peaks, which are found at 3.8 and 4.2 Å, whereas the triclinic $T//$ subcell [the symbol ($//$), indicates parallel] shows a series of relatively weak diffraction peaks with one dominating peak, which occurs near 4.6 Å.⁸ It is of course difficult to determine the chain packing subcell within the bilayer membranes of C_n -L-Ala-Azo- $C_{10}N^+$ because of their complicated chemical structure. However, according to the criteria described above, one dominating peak near 4.9 Å is considered to arise from a $T//$ subcell within the bilayers of the amphiphiles containing an odd number of carbons. On the contrary, the bilayers of the amphiphiles containing an even number of carbons contain two diffraction peaks near 3.8 and 4.2 Å, which indicates the presence of the $O\perp$ subcell arrangement. This consideration was supported by the FTIR study described below.

FTIR study

Because the strong absorption bands attributed to water are excluded, the FTIR spectra of the cast films were very easy to measure. Fig. 1 displays the FTIR spectra of the cast film bilayers of C_n -L-Ala-Azo- $C_{10}N^+$. All absorption bands changed in band shape, intensity and/or frequency with respect to whether the amphiphile possessed an even or an odd number of carbons. Marked differences between the two kinds of amphiphiles appeared in the CH_2 scissoring band and the amide absorption bands. Fig. 4 shows the CH_2 scissoring bands of C_n -L-Ala-Azo- $C_{10}N^+$ cast films at 25 °C. The peak contour of the CH_2 deformation band has been known to reveal the location of the *trans*-zigzag planes of the nearest-neighbouring chains, because the parallel and perpendicular alignments of the chain planes produce remarkably different patterns of band splitting due to interchain interactions.^{7,8} For example, the perpendicular alignments of the chains, which are peculiar within the $O\perp$ -type subcell, split the CH_2 scissoring band into 1473 and 1463 cm^{-1} components. The parallel alignments of the chains, which are plausible within the triclinic $T//$ -type subcell, give a singlet peak

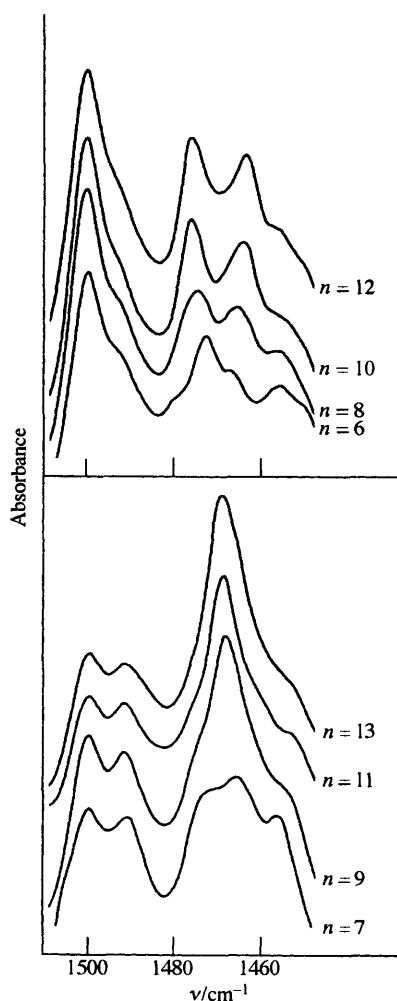


Fig. 4 The region of the CH₂ scissoring mode in the FTIR spectra of cast films from the aqueous bilayer of C_n-L-Ala-Azo-C₁₀N⁺ at 25 °C

at 1465 cm⁻¹. According to the splitting patterns, the amphiphiles of C_n-L-Ala-Azo-C₁₀N⁺ containing an even number of carbons possess perpendicular alignments of the chains, whereas the amphiphiles containing an odd number of carbons possess parallel alignments of the chains. The FTIR technique is very useful for determining the chain packing subcell within the bilayer aggregate unless the other band appears in the CH₂ scissoring region.¹²

The frequencies of the stretching and deformation bands of the amide group also changed with the number of carbons (Fig. 5). Because the bond energies of both the N-H and C=O bonds are weakened by the H-bond formation, the absorption frequencies of the stretching vibration in these functional groups should decrease. On the other hand, the absorption frequency of the N-H deformation band (amide II) increases with the H-bond formation, because it requires larger energy to deform the N-H bond, when the N-H bond is strained hard by the H bonding. Hence, the intermolecular H-bonding between the amphiphiles containing an even number of carbons is stronger than that between the amphiphiles containing an odd number of carbons.

Discussion

Bilayer structures

There are three possible structures for the bilayers of the amphiphiles of C_n-L-Ala-Azo-C₁₀N⁺, namely, a classic bilayer structure, a chain penetration structure and a fully interdigitated structure,¹³ whose lateral views are given in Table 4.

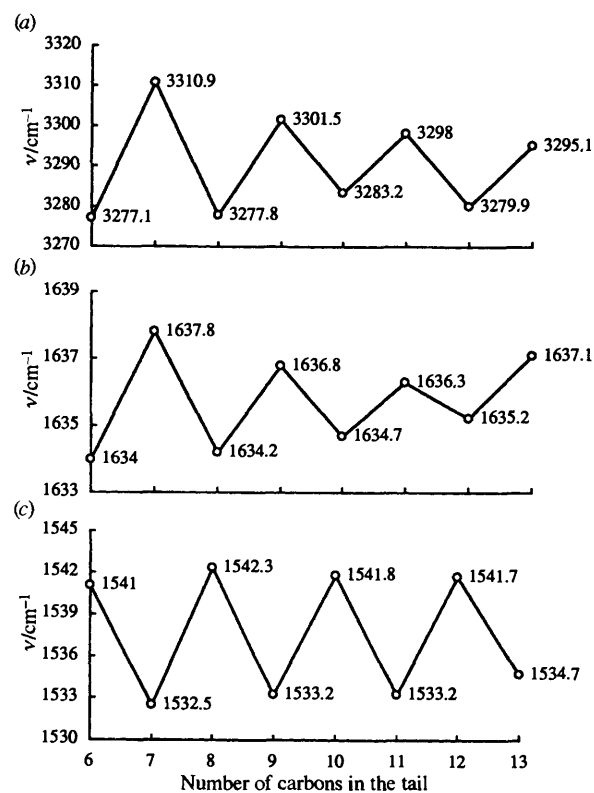


Fig. 5 Maximal wavenumbers of the (a) N-H, (b) amide I and (c) amide II bands within the FTIR spectra of the cast films

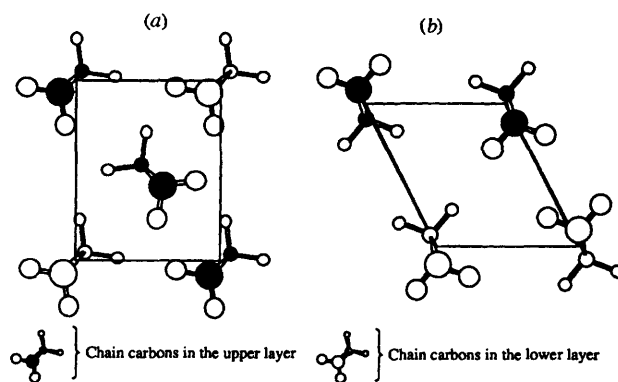


Fig. 6 Subcells in the chain penetration region; (a) The O \perp -type subcell within the bilayers of the amphiphiles containing an even number of carbons, (b) the T// type subcell within the bilayers of the amphiphiles containing an odd number of carbons

Within the chain penetration structure, the tail chains in one layer penetrate into the opposite layer. An advantage of the structure is to provide close packing of the tail chains, even if the sterically hindered methyl group of the alaninate residue is present. A disadvantage also exists. A gap may prevent close chain packing in the region between the head and the azobenzene group. However, the gap should not affect the bilayer formation, because triple chain ammonium amphiphiles, which adopt a classic bilayer structure, formed stable bilayer membranes despite a larger gap between spacers.¹⁴ We will thus discuss the variation in the absorption maxima of the bilayers of C_n-L-Ala-Azo-C₁₀N⁺ for the three possible structures.

Amphiphiles containing an even number of carbons. The hydrophobic chains containing an even number of carbons are packed according to the O \perp type subcell within the bilayer aggregate. The O \perp type subcell contains both the parallel and perpendicular alignments of the chain planes. Hence, a classic bilayer structure or a fully interdigitated structure could form a

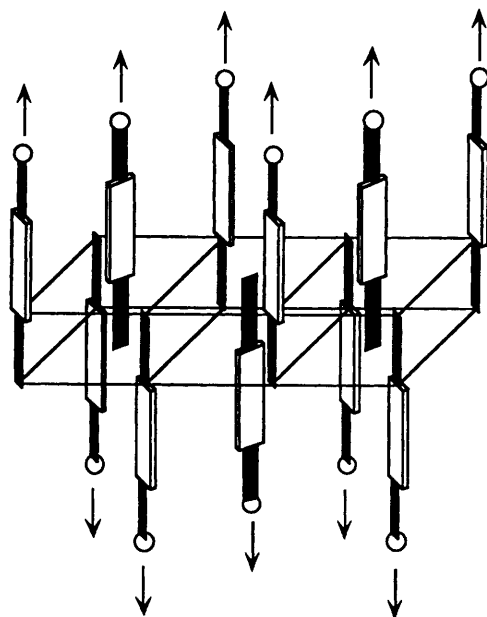


Fig. 7 Schematic illustration of the chain penetration structure formed from the amphiphiles containing an even number of carbons. Arrows indicate directions of respective molecules. Tilting has been neglected.

face-to-face packing of azobenzenes along either the a_s or b_s axis (s indicates a subcell). When the amphiphiles form a classic bilayer membrane, the angles of tilt of the molecules are calculated to be *ca.* 34° (Table 4). This angle of tilt is very favourable for the formation of the J aggregate which absorbs at 360–390 nm.¹⁵ In contrast, when the amphiphiles form a fully interdigitated structure, the tilt angles are calculated to be above 67° (Table 4). This tilting must yield the H aggregate which absorbs at *ca.* 300 nm. This is not consistent with the UV absorption (λ_{\max} 350 nm). We then assumed a characteristic chain penetration structure as shown in Figs. 6 and 7. In the structure, adjacent components alternately invert along the a_s and b_s axes (Fig. 6). The alternate inversion causes the loss of parallel stacking of the azobenzenes in one molecular layer and hence all the remaining planes of the nearest-neighbouring azobenzenes should align perpendicular to each other (face-to-side stacking) (Fig. 7). The perpendicular alignment of chromophores prevents an interchromophore interaction, giving rise to the absorption at 350 nm. The calculated bimolecular length in the chain penetration structure and the angle of tilt are given in Table 4.

Amphiphiles containing an odd number of carbons. The fully interdigitated structure is excluded from the possible structures because more than 17 \AA penetration reduces the calculated maximal thickness of the structure below the observed thickness. Thus, the classic bilayer structure and the chain penetration structure are possible. The angles of tilt within respective structures are given in Table 4. These angles are favourable for the formation of the H aggregate, because the bilayers of the amphiphiles containing an odd number of carbons possess the $T//$ -type subcell, which should provide parallel stacking of the azobenzene groups. However, λ_{\max} decreased with an increase in the chain length (Fig. 2). Because a less tilted structure absorbs at a shorter wavelength, the angle of tilt must increase with the chain length. Actually, the angle of tilt within the chain penetration structure enlarged with an increase in the chain length relative to a constant angle within the classic bilayer structure. This result means that the chain penetration structure is also plausible for the bilayers of the amphiphiles containing an odd number of carbons. However, we cannot rigorously exclude the classic bilayer structure in this case.

Hydrogen bonding

The different chain packing affected the mode of the intermolecular H bonding. As described before, the amphiphiles containing an even number of carbons formed stronger H bonding than those containing an odd number of carbons. The formation of the strong H bonding suggests that the adjacent molecules were not distant from each other. Hence, the absorption maxima at 350 nm does not result from a large distance between chromophores but from the perpendicular orientation of the chromophores. In fact, the amphiphiles containing an odd number of carbons can form intimate stacking of the chromophores (H aggregate) despite the rather weak H bonding. Although we cannot determine the conformation around the NH–CO linkage, the perpendicular alignments of the chain planes should provide favourable circumstances for formation of the H bonding.

Generality of the even-odd-chain effect

To our knowledge, such a drastic even-odd-chain effect as shown here has not previously been observed. However, a small difference between bilayers of amphiphiles containing an even and odd number of carbons has been reported. For example, the pre-transition temperatures (T_p) of the aqueous bilayers of acyl phosphatidylcholine with $n\text{-C}_{12}$ to -C_{19} acyl chains showed periodic change in the chain length, whereas the main transition temperature (T_c) linearly increased with the length of the chain irrespective of the number of carbon atoms.¹⁶ The aqueous bilayer membranes of the double chain amphiphiles such as N -(11-trimethylammoniumundecanoyl)- L -glutamate dialkyl ester with $n\text{-C}_{12}$ to -C_{16} alkyl chains [$\text{C}_{11}\text{-L-Glu-C}_{11}\text{N}^+$ ($n = 12\text{--}16$)] also showed no periodic change in the T_c but showed alternation of the absorption wavenumber in the IR spectra.¹⁷ Thus, although the double chain amphiphiles do not display a change in the T_c , all amphiphiles containing an even and odd number of carbons should form the bilayer membranes with different structures. In particular, as can be seen here, a difference in the chain packing causes a large difference in the properties of the bilayer membranes.

Conclusions

Bilayer-forming amphiphiles that contain an odd number of carbons in the tail have been neglected for a long period, because they are believed to be an extension of the amphiphiles containing an even number of carbons. However, the two kinds of amphiphiles behaved as entirely different species in the present case. The difference arose from the inherent chain packing within the respective bilayers. In order to explain the inherent chain packing, we proposed a new molecular arrangement, which we called a chain penetration structure. So far the chain packing has not been extensively discussed. This is because the traditional bilayer structures necessarily contain parallel alignments of the chromophore planes, even if an $O\perp$ type subcell is formed. However, within the chain penetration structure, the orientation of chromophores is dependent upon whether the *trans*-zigzag planes of the tail chains are parallel or perpendicular. In particular, every other inversion of components causes a loss of parallel alignments of the chromophore planes. In this case, a simple lateral view of the bilayer varies with the angle of the perspective. We therefore emphasize that bilayer properties must be considered three-dimensionally.

References

- 1 T. Kunitake and Y. Okahata, *J. Am. Chem. Soc.*, 1977, **99**, 3860.
- 2 T. Kunitake, *Angew. Chem., Int. Ed. Engl.*, 1992, **31**, 709; J.-H. Fuhrhop and J. Köning, *Membranes and Molecular Assemblies: The Synergetic Approach*, The Royal Society of Chemistry, Cambridge, 1994; J. B. F. N. Engberts and D. Hoekstra, *Biochim. Biophys. Acta*, 1995, **1241**, 323.

- 3 N. Yamada, T. Sasaki, H. Murata and T. Kunitake, *Chem. Lett.*, 1989, 205.
- 4 N. Yamada and M. Kawasaki, *J. Chem. Soc., Chem. Commun.*, 1990, 568.
- 5 M. Shimomura, R. Ando and T. Kunitake, *Ber. Bunsenges. Phys. Chem.*, 1983, **87**, 1134.
- 6 N. Nakashima, R. Ando and T. Kunitake, *Chem. Lett.*, 1983, 1577; Y. Wakayama and T. Kunitake, *Chem. Lett.*, 1993, 1425.
- 7 R. G. Snyder, *J. Mol. Spectrosc.*, 1961, **7**, 116; R. G. Snyder, *J. Chem. Phys.*, 1979, **71**, 3229.
- 8 N. Garti and K. Sato, *Crystallization and Polymorphism of Fats and Fatty Acids*, Marcel Dekker, 1988.
- 9 P. P. Cohen and R. W. McGilvery, *J. Biol. Chem.*, 1946, **166**, 261.
- 10 N. Nakashima, K. Morimitsu and T. Kunitake, *Bull. Chem. Soc. Jpn.*, 1984, **57**, 3253.
- 11 *Org. Synth.* Coll. Vol. 3, 1955, 382, John Wiley & Sons, Inc.
- 12 H. H. Mantsch, V. B. Kartha and D. G. Cameron, *Surfactant in Solution*, ed. K. L. Mittel, Plenum Press, New York, 1983, pp. 673.
- 13 T. Nishimi, Y. Ishikawa, T. Kunitake, M. Sekita, G. Xu and K. Okuyama, *Chem. Lett.*, 1993, 295; Y. Ishikawa, T. Nishimi and T. Kunitake, *Chem. Lett.*, 1990, 165; K. Okuyama, M. Ikeda, S. Yokoyama, Y. Ochiai, Y. Hamada and M. Shimomura, *Chem. Lett.*, 1988, 1013; K. Okuyama, Y. Ozawa and T. Kajiyama, *Nippon Kagaku Kaishi*, 1987, 2199.
- 14 T. Kunitake, N. Kimizuka, N. Higashi and N. Nakashima, *J. Am. Chem. Soc.*, 1984, **106**, 1978.
- 15 G. Xu, K. Okuyama and M. Shimomura, *Bull. Chem. Soc. Jpn.*, 1991, **64**, 248; K. Okuyama, C. Mizuguchi, G. Xu and M. Shimomura, *Bull. Chem. Soc. Jpn.*, 1989, **62**, 3211.
- 16 R. Silvius, B. D. Read and R. N. McElhaney, *Biochim. Biophys. Acta*, 1979, **555**, 175.
- 17 N. Yamada and Y. Koyama, unpublished results.

Paper 6/03325C

Received 13th May 1996

Accepted 2nd September 1996